Structure and Hydrogen Bonding in Liquid and Supercritical Aqueous NaCl Solutions at a Pressure of 1000 bar and Temperatures up to 500 °C: A Comprehensive Experimental and Computational Study

G. V. Bondarenko,[†] Yu. E. Gorbaty,*[,†] A. V. Okhulkov,[†] and A. G. Kalinichev*[,†,‡]

Institute of Experimental Mineralogy, Russian Academy of Sciences, Chernogolovka, Moscow Region, 142432 Russia, and Department of Geology and NSF Water CAMPWS, University of Illinois at Urbana-Champaign, 1301 West Green Street, Urbana, Illinois 61801

Received: July 7, 2005; In Final Form: January 8, 2006

The behavior of aqueous 1.1 M NaCl solution at a constant pressure of 1000 bar in the temperature range 25−500 °C has been studied with the use of IR absorption, Raman scattering, X-ray diffraction, and molecular dynamics (MD) simulations. The results are compared with the data for pure water under identical external conditions. The main purpose of the experimental and theoretical studies was to understand in what way an electrolyte dissolved in water influences the hydrogen bonding and structural features of water. As was found, the vibrational spectra show no essential difference between the properties of solution and pure water. However, the experimental pair correlation functions and the results of MD simulations present an evidence for very different nature of these substances. A characteristic feature of the structure of NaCl solution is a considerable contribution of strong $O-H\cdots Cl^-$ bonds. As the temperature increases, the number of such bonds decreases partially due to a phenomenon of ion pairing, so that at high temperatures the properties of the solution become closer to the properties of water.

1. Introduction

Aqueous electrolyte solutions have always attracted much attention because of their crucial importance in many natural and industrial processes. On one hand, our entire planetary environment is the result of enduring and tenacious work of hot compressed aqueous solutions that have transformed the Earth's crust, given birth to the oceans, created ore deposits and soil, and were responsible for the origin of life and the development of the human civilization itself. On the other hand, practical significance of the supercritical electrolyte aqueous solutions is appreciably growing in recent years, because of their ubiquitous use in many traditional industrial applications and especially due to the new opportunities provided by the use of supercritical fluids to create "clean" or "green" environment-friendly chemical technologies.[1,2]

Nevertheless, it has to be admitted that not very much is known of the molecular behavior of electrolyte solutions under high pressures and temperatures. It is, for example, very important to understand in what way such thermodynamic parameters as pressure, temperature, and the concentration of dissolved electrolytes affect the most characteristic feature of any aqueous system—hydrogen bonds between H_2O molecules. The phenomenon of H-bonding is the most important factor determining the physical and chemical properties of water and aqueous solutions. In this work we have undertaken a study of 1.1 M aqueous solution of NaCl with the use of IR absorption, Raman scattering, X-ray diffraction, and MD computer simulations in the temperature range from 20 to 500 °C and at a constant supercritical pressure of 1000 bar.

In the recent years, many results on a variety of similar electrolyte solutions using these techniques have already been obtained.[3−22] However, they are often difficult, if not impossible, to compare because of the different concentrations, different ranges of temperature and pressure, and very different quality of data. To the best of our knowledge, the simultaneous use of several complementary experimental and computational methods for the study of electrolyte solutions at the same concentration and at the same thermodynamic parameters has been performed for the first time.

Following the widespread ideas,[4] we might think that at a chosen concentration (2 molecules of NaCl per 100 molecules of water) about a quarter of all water molecules might be expected to reside in the coordination shells of ions or at least be in a close proximity to them. At larger concentration, the coordination shells may adjoin each other, so that the intrinsic infinite network of hydrogen-bonded water molecules ceases to exist. We assume that at the chosen concentration, the infinite H-bonding structure remains in place still, but the local molecular-level structure and properties of the solution may differ quite noticeably from those of pure water. Even a couple of decades ago, it seemed to be certain that the mechanisms of ionic hydration had been understood to such a perfection that one can distinguish between "water structure breaking" and "structure making" ions.[23] The only embarrassing thing about confidently applying such definitions is the lack of molecular-level understanding what the structure of water is and what, in general, the very term "structure" means, as applied to liquids.[24] Most early theories of the structure of aqueous solutions were based on simplified, rather than crystallographic, concepts. They, perhaps, can still be used as an initial approximation, but they are hardly adequate to properly describe the real, far more complicated, incessantly varying picture of molecular rearrange-

* Corresponding authors. Yu.E.G.: e-mail, hunch@iem.ac.ru. A.G.K.: e-mail, kalinich@uiuc.edu.
[†] Russian Academy of Sciences.
[‡] University of Illinois at Urbana-Champaign.

10.1021/jp0537198 CCC: $33.50 © 2006 American Chemical Society
Published on Web 03/01/2006

ments and motions in water. The same can be said about the more recent theories. It is quite possible that a complete understanding of the structure of aqueous systems will never be reached. Is it necessary though? It seems more reasonable to focus on the phenomena of practical importance and to approach the problems step by step. For that we need to accumulate more experimental data, in particular at high temperatures and pressures. To begin with, it would be useful to understand, to what extent the dissolution of a typical electrolyte in water affects the temperature evolution of H-bonding network in water. We believe that the methods used in this work allow us to achieve this goal. Vibrational spectroscopy (sections 2 and 3) is a very sensitive probe for measuring the extent of hydrogen bonding and the energetics of H-bonding, whereas the pair correlation functions obtained from X-ray diffraction data and MD computer simulations (sections 4 and 5) can provide quantitative understanding of the spatial arrangements of the H_2O molecules and ions in the solution.

2. IR Absorption Spectroscopy

The symmetric (ν_1) and asymmetric (ν_3) stretching vibrations of H_2O are very sensitive to the local H-bonding environment in the O−H···O systems.[25] However, the absorption bands corresponding to these vibrational modes are strongly overlapped, so that it is practically impossible to distinguish an individual mode in the total, very broad and complicated, absorption band. So far, nobody can be quite sure of any suggested interpretation of the band. The situation becomes easier, if the spectra of HDO are considered. In this case, the stretching modes ν_{OH} and ν_{OD} are separated from each other by ~1000 cm^{-1}. To recognize the difference in the behavior of ν_{OD} in the spectra of water and NaCl solution, our IR experiments have been carried out with a mixture of 3 mol. % of HDO in H_2O.

2.1. Experimental Details. Triply distilled water was used to prepare the solvent and the solutions. D_2O (99.8%), necessary to prepare the H_2O/HDO mixture, was obtained from "Isotop" (Russia), and NaCl of spectral purity was from "Khimreaktiv" (Russia). A unique high-pressure high-temperature optical cell with variable path length[26,27] was used to obtain the spectra. The cell and the specially developed measuring technique allow one to significantly increase the accuracy of the experiments. In the case of a classic wave-dispersive spectrometer, we have to obtain two spectra $T_1(\nu)$ and $T_2(\nu)$ for H_2O with a difference of path lengths Δ_1. However, the absolute values of path lengths cannot be accurately known because of the deformation of the cell parts due to the high stress and thermal expansion at high temperatures and pressures. Nevertheless, the difference Δ between the path lengths in two consecutive runs at the same temperature and pressure can be measured with the sufficient accuracy. For the mixture of HDO in H_2O we must collect another pair of spectra $T_3(\nu)$ and $T_4(\nu)$ at a difference of path lengths Δ_2. Then the absorption coefficient is calculated as

$$\kappa_{HDO}(\nu) = \frac{\ln[T_4(\nu)/T_3(\nu)]}{c_{HDO}\Delta_2} - \frac{Mc_{H_2O}\ln[T_2(\nu)/T_1(\nu)]}{\rho c_{HDO}\Delta_1} \quad (1)$$

where κ_{HDO} is the absorption coefficient, c_{HDO} is the mole concentration of HDO, c_{H_2O} is the concentration of H_2O, M is the molecular weight of H_2O, and ρ is the density at given T and P.[28−31] The algorithm of data processing has been described in detail elsewhere.[26,27] With the single beam FTIR instruments, we still have to measure four spectra: two background spectra and two sample spectra.

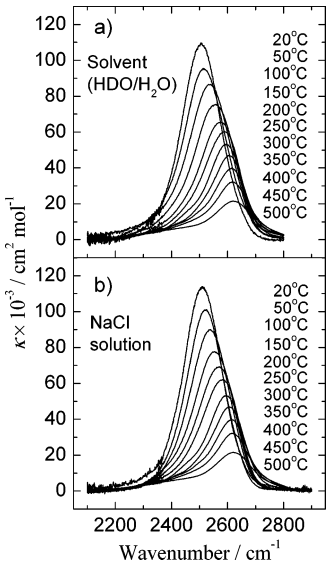

Figure 1. (a) IR spectra of HDO/H_2O mixture at isobaric heating. (b) Same of NaCl solution.

The same measuring procedure should be applied to the pure water and to the NaCl solution at exactly the same temperatures and pressures. Thus, to compare the spectra of ν_{OD} for the solvent and solution, we have to obtain eight spectra. This laborious experimental technique requires high reproducibility of measurements, which our cell with the variable path length can provide. The spectra of the absorption coefficient had been processed with the usual procedures, such as baseline correction, offset, and, if necessary, smoothing. All the spectra were processed in exactly the same way. The most difficult part of the experiment was the measuring of Δ, which for water at low temperature and high pressure amounts to only a few micrometers. The procedure of obtaining Δ has been described in detail elsewhere.[27] Most of the measurements were made with the use of the Perkin-Elmer mod. 983 spectrometer. Several experiments were also made with the Thermo Nicolet FTIR spectrometer Avatar 320.

2.2. Results and Discussion. Figure 1 shows the spectra of the solvent (3 mol % HDO in H_2O) and those of NaCl solution obtained at a constant pressure of 1000 bar and at temperatures up to 500 °C. The behavior of the spectra in both series is very much alike. As might be expected, the increase in temperature causes the shift of the band position to higher wavenumbers and a strong decrease in the intensity of absorption. This is an unmistakable indication of the significant weakening of hydrogen bonding in both systems with the increase of temperature.[25] It should be also noted that no features, such as shoulders, inflection points, etc., are observed in the spectra, which could have been interpreted in favor of an uneven, discrete energy distribution in the H-bonding network. One can see, however, that the contour of the band becomes more asymmetrical at higher temperatures.

The intensity of IR absorption due to OH and OD vibrations is known to be very sensitive to the energy of hydrogen bonding.[32,33] It is 25−30 times smaller for the low-density vapor, in which the amount of H-bonded states is very low, than for ice with all possible hydrogen bonds realized. Therefore, if there is a difference in the character of hydrogen bonding between the solvent and solution, it should be noticeable in the behavior of the integrated intensity A of absorption, which has been calculated from the experimental spectra as

$$A = \Delta\nu \sum_{2100}^{2800} \kappa(\nu) \tag{2}$$

where $\Delta\nu$ is the increment of the two-dimensional $\kappa(\nu)$ array. The temperature trends $A(T)$ for the solvent and solution are shown in Figure 2a. As can be seen, the scatter of experimental points is fairly low. The accuracy of these data is estimated as $\pm 7\%$. One can see that the difference in the behavior of $A(T)$ between the solvent and NaCl solution is very small. Both curves diverge most noticeably at room temperature but the difference in A values is only about 10%, whereas in both cases A decreases approximately by factor 3.8 in the whole temperature range explored. It is important to emphasize that the measured IR intensities were corrected for the density of water and the solution (eq 1), which vary with temperature somewhat differently. (The density data were taken from the literature for pure water[31] and aqueous NaCl solutions.[28−30] See also Figure 13a below). Taking into account this density correction, we can conclude that the larger absorption intensity for the solvent (for the sake of simplicity we hereafter call it "water") apparently means that the H-bonding energy is higher than in the solution. Yet, at temperatures above 200−250 °C, the situation is reverse—the H-bonds energy in the solution exceeds that in water. Such an inference is, however, not very reliable because the difference in the temperature trends for water and solution is at the limits of our estimated experimental error. On the other hand, the trend for the stretching band position ν_{max} (OD) seems to confirm this inference. Although the shift of the band due to hydrogen bonding is a less sensitive characteristic than the intensity of absorption, it can be measured with much better accuracy. In the described experiments, it was not worse than ± 3 cm^{-1}. As seen in Figure 2b, the red shift is smaller for the solution at room temperature and greater at high temperatures. Therefore, the behavior of ν_{max} (OD) corresponds to the temperature trend for the intensity of absorption. Then again, the discrepancy between temperature trends for water and solution lies practically within the range of experimental error.

Looking at Figure 1, one can notice that at low temperatures the spectra of water appear broader than those of the NaCl solution are. Figure 3 shows this distinctly, but again, the difference is not that large. More interesting is the nontrivial temperature dependence of the band half-widths. Figure 2b demonstrates that the band position changes monotonically as temperature increases. According to the commonly accepted rule of a strong and practically linear correlation between ν_{max} (OD) (or ν_{max} (OH)) and the half-width of the band,[32,33] the half-width should change monotonically as well. Then why do the temperature trends in Figure 3 exhibit both maxima and minima?

The increase in the half-width at supercritical temperatures can be easily explained. It has already been shown[24,34] that above the critical temperature, free (inertial) rotation of water molecules becomes possible. This leads to the broadening of the stretching band with increasing temperature, and at a lower density, to the emergence of the unresolved P-, Q-, and R-rotational branches. The maximum half-width observed at 100−150 °C is more difficult to explain. In our opinion, it presents clear evidence for the existence of different local structural environments of water molecules, or "structural species". Although the energy distribution for each of these species is very broad, they are, nevertheless, in thermodynamic equilibrium. As the temperature increases, the amount of strongly bonded species diminishes and the quantity of the weakly bonded species tends to grow. Because of the significant breadth of the distributions, the individual components contributing to the contour of the stretching band are not resolved. However, the positions of these components differ, so the change in the ratio of component abundances results in the maximal half-width of the total contour as the maximal intensities become approximately equal. Of course, this does not mean that the abundances of species also become equal, because the absorption coefficients for the dissimilar species are different. The validity of this interpretation is confirmed further by the X-ray scattering data (see section 4).

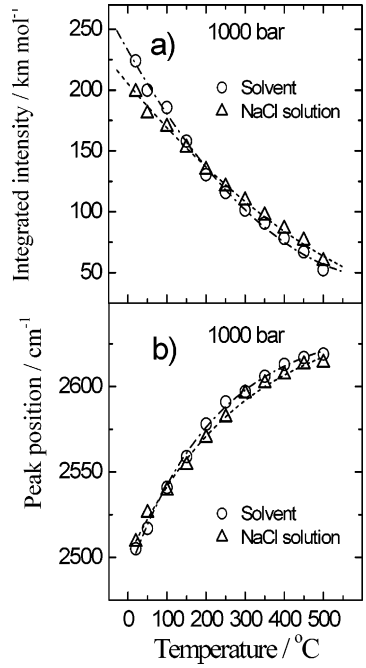

Figure 2. (a) Temperature dependence of the integrated intensity of absorption for the solution and solvent at isobaric heating. (b) Temperature dependence of the maximum peak position.

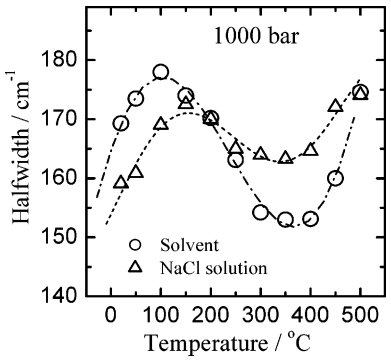

Figure 3. Temperature trends of the IR spectral band half-widths for HDO/H_2O solvent and NaCl solution. Lines are guides for the eye.

Here is a good opportunity to make clear one important point. Numerous maxima and minima were discovered on the temperature or pressure dependences of various water properties. The most hackneyed example is the density maximum at 4 °C. Very often such features are interpreted in terms of a cardinal change of the water structure. In fact, nothing of the kind occurs at the temperatures or pressures corresponding to the extrema. All these features, including the maximum of the half-width, *are merely quantitative consequences* of the continuous competitive processes, which accompany the weakening or strengthening of hydrogen bonding.

Concluding this section, we would like to emphasize that the difference in the behavior of IR spectra of pure water and NaCl solution at heating to high temperatures is unexpectedly small.

Discussing the energy of H-bonding, we have to remember that, in the case of water, the integrated intensity of absorption A reflects only the state of hydrogen bonds O−D···O. However, in the case of the NaCl solutions, it also involves interaction of the O−D groups with the anions.[35−37] One can assume then that the energy of interaction of OD groups with the ions is comparable with the energy of hydrogen bonds. If this is the case, it is difficult to draw definite conclusions from the discussed results. The presence of Na^+ cations, of course, also perturbs the H-bonding network. However, unlike the anions in the solution, the cations are not directly coordinated by the hydrogen atoms of H_2O molecules due to their electrostatic repulsion. Thus, the effects of cations on the O−D stretching vibrations are expected to be much weaker than those of the anions, and we do not observe such effects in our spectra. The effects of the cationic and anionic hydration on the water structure and H-bonding are discussed in more detail in section 5 below in conjunction with the MD simulation results.

3. Raman Scattering

IR spectroscopy is a more informative technique than the spectroscopy of Raman scattering because it is a quantitative method allowing one to work with absolute intensities. However, the spectral range accessible for IR spectroscopy with the use of high-temperatures high-pressures optical cells is restricted to 2000 cm^{-1} by the transparency of sapphire, the most commonly used material for optical windows. Raman spectroscopy has no such limitation. Therefore, we can use it to probe if there are any perceptible differences between the solvent and solution in the full spectral region.

3.1. Experimental Details. The same 1.1 M NaCl solution was studied by Raman scattering, but instead of the HDO/H_2O mixture, pure H_2O had been used as a solvent. The Raman spectra in the region 200−4000 cm^{-1} were obtained with the use of the Renishaw RM1000 Raman spectrometer equipped with Ar^+ ion laser emitting at 514 nm. A miniature optical cell with one sapphire window (using 180° geometry) had been developed for high-temperature high-pressure studies of liquids and supercritical fluids.[27] The laser beam was directed into the cell with the standard Renishaw angular accessory attached to the nosepiece of the microscope. The spectra were obtained at the same thermodynamic states as the IR spectra discussed above.

The Raman spectroscopy of fluids at high temperatures is very often complicated due to a very troublesome phenomenon of fluorescence that arises above 200−250 °C. The fluorescence grows with increasing temperature, so that at 400−500 °C a weak Raman spectrum is, most frequently, completely "obscured" by the noise from the very intense spectrum of fluorescence. The origin of this effect is not clearly known, but the most likely reason for it is the presence, in minuscule amounts, of some organic impurities that cannot be totally removed from water with the usual means, such as distillation, ion-exchange, etc. These impurities undergo thermal decomposition resulting in the fluorescing species. We have found that this undesirable effect can be reduced by long exposure of a sample to temperatures above 500 °C. For this purpose an electric pump was included in the high-pressure line, forcing the sample fluid to circulate at a pressure of about 300 bar through the whole system, including the hand pump and the cell heated to 530−550 °C. The process was monitored by collecting the spectra until the fluorescence background became acceptable. The cell was then cooled to room temperature, pressurized again with the hand pump, and the normal experiment was started. Despite these precautions, some remnants of the florescence were present in the high-temperature spectra, so the spectra had to be carefully baselined. All the spectra were normalized to the density of the sample at a given temperature and pressure.[28−31]

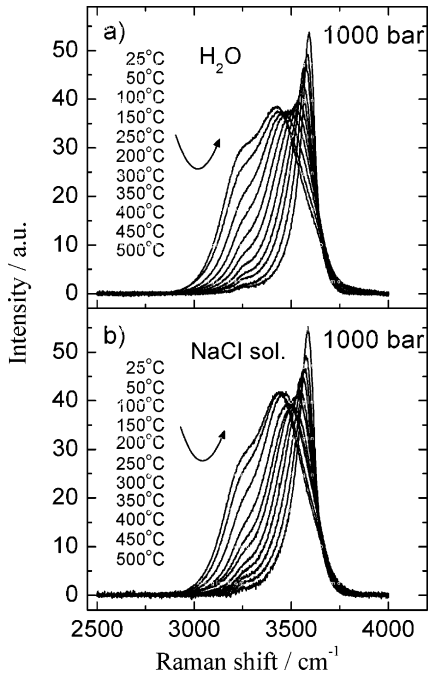

Figure 4. (a) Raman spectra of water at isobaric heating. (b) Same for NaCl solution.

3.2. Results and Discussion. To our disappointment, we were unable to find any difference in the temperature behavior of the Raman spectra of NaCl aqueous solution and pure water in the spectral range 200−2100 cm^{-1} unavailable with our IR cell. Perhaps, it is not surprising because no serious difference is also seen between the spectra of solution and pure water in the region of stretching modes presented in Figure 4. However, exactly as in the case of IR absorption, the spectral bands of NaCl solution at low temperatures seem less broad than the spectra of pure water. In contrast, at high temperature the remaining band is narrower in water.

The spectra in Figure 4 are hard to interpret. It is commonly thought that the contour of the stretching band in the spectrum of dense water is composed of the ν_1, ν_3 modes, and the overtone $2\nu_2$ enhanced by the Fermi resonance with ν_1.[36] Due to the effect of hydrogen bonding, individual components of the total contour are very broad and overlap each other. Discussing the half-width of the ν_{OD}(HDO) (Figure 3), we have seen that the contour of this isolated uncoupled band is, most likely, complex, reflecting the equilibrium between at least two energetically distinct species. Obviously, the same should be observed for each component of the total stretching band of H_2O. In addition, nonuniformly bonded water molecules may have different symmetry, thus influencing intensities, widths, Fermi resonance, in short, making the interpretation of the band shape much less straightforward. We believe, therefore, that numerous attempts to apply a simple curve fitting procedure to the complicated contour of the stretching band can only serve very limited purposes.

The position of band maximum ν_{max} (Figure 5b) is the only distinct characteristic one may rely upon, when comparing the Raman spectra of pure water and NaCl solution. As can be seen, the temperature trends for ν_{max} are very similar to those for ν_{OD}(HDO) (Figure 2b). Moreover, the difference in the tem-

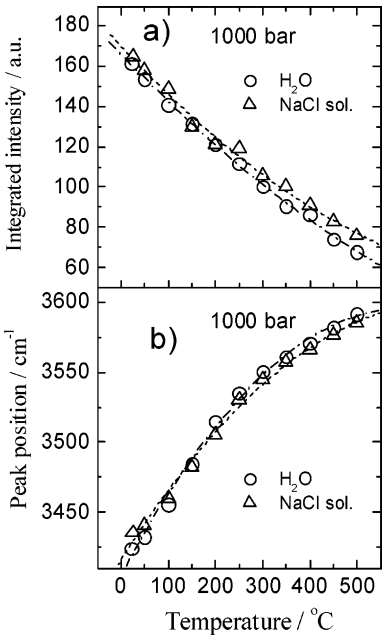

Figure 5. (a) Temperature behavior of integrated intensity of Raman scattering at isobaric heating. (b) Same of maximum peak position.

perature trends for water and the solution is consistent with what is deduced from the IR spectra: at low temperatures, the H-bonding is stronger in pure water, and at high temperature, the situation is reversed. But again, the differences are nearly within the estimated error bounds.

To what extent the degree of hydrogen bonding in the system affects the Raman intensity of the stretching band is not known for certain. This is because the absolute intensities (scattering cross-sections) are practically impossible to obtain. In addition, it is hardly possible to find a suitable substance for use as an internal standard that would not react with the supercritical water or solution or remain stable under the conditions of our experiments. It is believed that the integrated intensity of Raman scattering decreases as hydrogen bonding weakens, but this effect is, apparently, less pronounced than in the case of the intensity of IR absorption. In the temperature range 25−500 °C the integrated intensity of the ν_{OD}(HDO) IR adsorption band (Figure 2a) decreases by a factor of 3.8, whereas the intensity of Raman scattering (Figure 5a) decreases only by a factor of 2.3. Figure 5a shows that the intensities of the stretching band in the solution and pure water coincide within the limits of experimental error.

4. X-ray Scattering. Molecular Pair Correlation Functions

Data on the intensity of X-ray scattering have been obtained at the isobaric heating of 1.1 M NaCl solution up to 500 °C at a constant pressure of 1000 bar. Preliminary results of this study have been already published.[38] Here we are going to discuss the results in more detail and in conjunction with the spectroscopic and MD data (section 5).

4.1. Experimental Details. The raw data on the intensity of scattering were obtained using the energy-dispersive X-ray diffraction technique (EDXD).[39] The main advantage of the method, as applied to high-pressure high-temperature X-ray scattering experiments, is the possibility to use narrow (0.1−0.3 mm) collimating slits in the body of a high-pressure cell instead of large-aperture windows. The technique also provides high statistical accuracy at reasonable exposure times (in our experiments, typical exposure times were 15−20 h, depending on the density of the solutions). A high-pressure high-temperature EDXD cell for X-ray diffraction experiments has been described elsewhere[40] along with the basic algorithms and procedures of data processing.[41−43] The only difference in the raw data treatment for the present set of measurements was that the Na and Cl atom form factors[44] were introduced in addition to the molecular form factor of water[45] in the calculations of the structure functions. It is also worth mentioning that the important procedure of eliminating the truncation errors was based on the extrapolation of the "tail" of the structure function to infinity.[46]

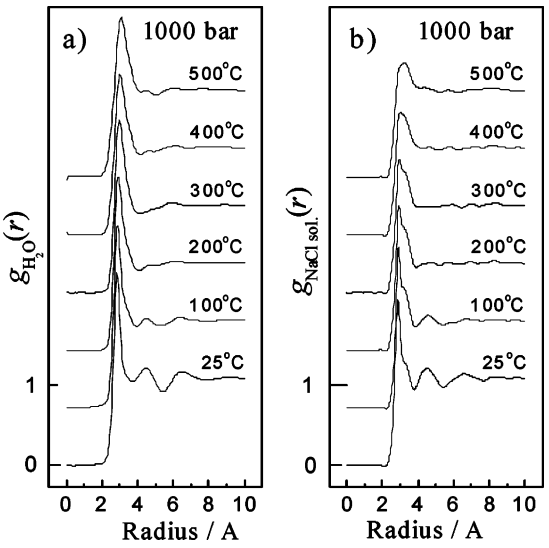

Figure 6. (a) Pair correlation functions of water at isobaric heating. (b) Pair correlation functions of NaCl solution at the same parameters of state.

4.2. Results and Discussion. The pair correlation functions (PCF) of water and NaCl aqueous solution are presented in Figure 6a,b. One can see that, unlike IR and Raman spectra, PCF of these two substances look entirely different. The first narrow peak of $g(r)$ of H_2O at 2.82 Å (Figure 6a) corresponds to the separation between hydrogen-bonded water molecules. Pairs of nonbonded or weakly bonded molecules reveal themselves as an excessive correlation at about 3.2−3.3 Å.[24,47] The next peak at ∼4.5 Å is an indication of tetrahedral ordering in liquid water. It corresponds to the distance between the vertexes of a tetrahedron formed by four nearest-neighbor H_2O molecules, two of which accept H-bonds from the central molecule, and two other donate H-bonds to it. The function $4\pi r\rho_0 g(r)$ of water can be very well approximated by three Gaussians in the region 2−4.5 Å (see, e.g., ref 47 and Figure 8 below). As the temperature increases, the area under the first Gaussian (hydrogen-bonded molecular pairs) decreases while the area under the second Gaussian (nonbonded pairs) simultaneously grows up. This simple interpretation had allowed us to find the temperature dependence of the extent of hydrogen bonding in water.[47]

In pure water, only three *partial* PCF $g_{O-O}(r)$, $g_{O-H}(r)$, and $g_{H-H}(r)$ are contributing to the total molecular $g(r)$ of the fluid. Moreover, because the X-rays scatter much more strongly by the oxygen atoms in this system, the two latter functions contribute very little to the total $g(r)$, so that it may be actually considered as a proxy for $g_{O-O}(r)$. The interpretation of the total $g(r)$ in the case of NaCl aqueous solution is much less straightforward, because in this case the total PCF consists of 10 partial correlation functions. Even if the interactions with hydrogen atoms would be excluded, at least 6 partial $g_{ij}(r)$ contribute to the full $g(r)$ with a significant weight. This makes detailed peak assignments for the $g(r)$ functions presented in

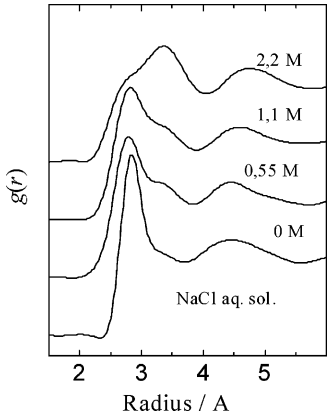

Figure 7. Correlation functions of NaCl aqueous solution at different concentrations. Ambient conditions.

Figure 6b very problematic. MD computer simulations may to some extent help to solve this problem because all partial $g_{ij}(r)$ functions are easily calculated using this technique. The results of the MD simulations will be discussed in the next section. Here we rely only on the typical interatomic separations to understand the experimentally obtained $g(r)$ of the aqueous NaCl solution.

As is seen in Figure 6b, the most distinct difference between $g(r)$ of water and solution is observed in the narrow region of distances near 3.2−3.3 Å. For the solution at low temperatures, a well-defined shoulder is observed, and its intensity increases with the temperature rise. At 500 °C, this feature prevails over the first peak corresponding to the nearest O−O distances. It is hardly possible that the only reason for such a behavior is the increased amount of the weakly bonded H_2O neighbors, because the comparisons of vibrational spectra of water and solution do not indicate any considerable difference in the energy of bonding. Therefore, the feature is undoubtedly associated with the Na^+ and Cl^- ions in solution. Figure 7 shows $g(r)$ of NaCl solutions obtained at different concentrations. Here the shoulder at about 3.3 Å increases with concentration and at 2.2 M turns into a principal peak. In good agreement with the literature data[4] the first peak of MD calculated $g_{Cl-O}(r)$, corresponding to the nearest separation between these two atoms, is positioned at ∼3.2 Å. It is unlikely that O and Cl^- interact directly. Instead, they are part of a configuration O−H···Cl^-, which sometimes is also called a hydrogen bond. MD calculations show that the Cl^-···H separation is distributed around 2.3 Å, and the length of the O−H bond is on the order of 1 Å. The sum of these distances is 3.3 Å, which means that the configuration O−H···Cl^- is close to linear (the average O−H···Cl^- angle is ∼162°). One ought to remember, however, that these are values calculated from MD simulations, which may differ somewhat from the actual interatomic distances in real solutions. On the other hand, good agreement between experimental (2.82 Å) and calculated (2.75 Å) values for the shortest O−O separation implies that the difference between the theory and experiment for other pair correlations should not be large.

Thus, the only interactions that may be observed in the region around 3.3 Å are O−Cl (most likely, O−H···Cl^-) and O−O for nonbonded or weakly H-bonded H_2O molecules. In the region corresponding to the first coordination shell, the radial distribution function of molecular density $D(r) = 4\pi r^2\rho_0 g(r)$, where ρ_0 is the average density, may be presented as a sum of two overlapping components. For pure water $D(r)$ simply represents the H-bonded and nonbonded molecular pairs, but in the case of NaCl solution this part of $D(r)$ is of a more complex nature.

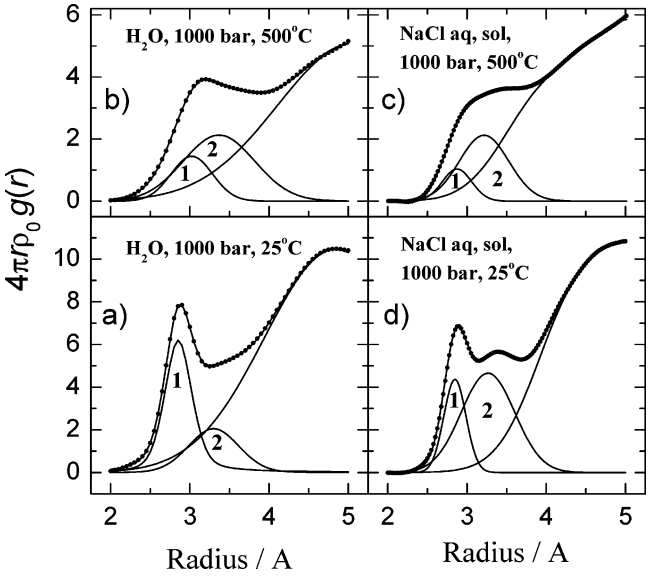

Figure 8. (a) and (b) Examples of the curve fit procedure for RDF of water. (c) and (d) Same for NaCl solution. See explanation in text.

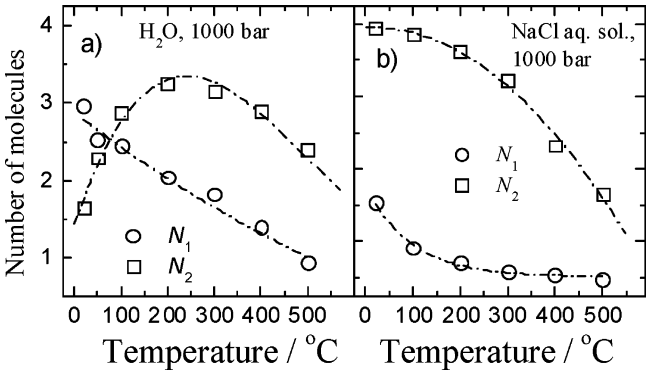

Figure 9. (a) Temperature trends for dissimilar molecules in the first coordination sphere of water. (b) Same for NaCl solution.

To estimate the number of water molecules belonging to each component, one may use a curve fitting procedure, which is more correct to apply to the function $D(r)/r = 4\pi r\rho_0 g(r)$. It has been previously shown that for such a function the shape of the components is close to Gaussian.[43] The amplitude of a Gaussian peak being multiplied by r thus presents a number of molecules in the corresponding component of $D(r)$. Figure 8 shows some examples of the curve fitting of $D(r)$ for pure water and the NaCl solution. Because the peaks of the distributions are not very well resolved, the fitting procedures must be used very cautiously. Sometimes the problem may not have a unique solution. In fact, we could obtain as good a fit as that in Figure 8 with slightly different parameters for individual components. Therefore, to achieve the most consistent results, we always repeated the procedure many times, using different initial parameters. The aim was not only to achieve the best fit but also to provide more or less smooth and consistent temperature trends for all the parameters of the deconvolution (positions, widths and amplitudes of the Gaussian components) over the entire temperature range studied for both pure water and the NaCl solution. The areas under individual peaks shown in Figure 8 correspond to the average number of molecules in the first coordination sphere. Figure 9a,b demonstrates how the quantities of recognizable structural species change with temperature. Here N_1 corresponds to the peak of $D(r)$ centered at ∼2.8 Å (H-bonded nearest neighbors) and N_2 to the peak at about 3.2−3.3 Å (nonbonded or weakly bonded nearest neighbors).

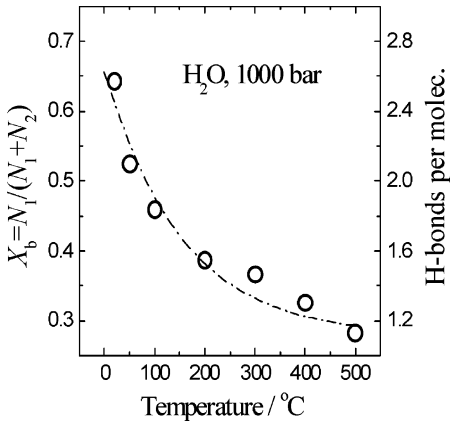

Figure 10. Temperature dependence of the mole fraction of bonded molecules X_b in pure water.

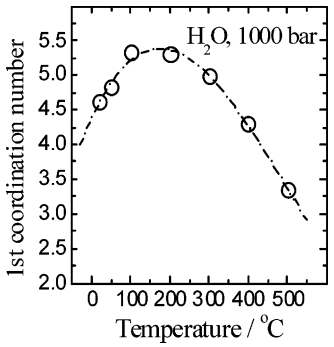

Figure 11. Temperature behavior of the first coordination number of water.

Comparing the vibrational spectra of pure water and NaCl solution, we might have assumed that there was no substantial difference in the intermolecular interactions and temperature behavior between these two systems. Contrary to this observation, the results of X-ray scattering experiment present a strong evidence to consider them as structurally quite different substances. Let us try to understand first what is going on in water as temperature increases. At room temperature, the average number of H-bonded molecules N_1 surrounding each H_2O molecule exceeds the number of nonbonded (or weakly bonded) molecules N_2. The fraction of bonded molecules $X_b = N_1/(N_1 + N_2)$ is 0.65. As the temperature increases, N_1 diminishes while N_2 grows. Above 250 °C the number of nonbonded molecules in the first coordination sphere begins to decrease simply because of the decreasing density along an isobar. Figure 10 shows the temperature behavior of X_b at a constant pressure of 1000 bar. The scale on the right shows the average number of hydrogen bonds per molecule, which is defined as $4X_b$. These data somewhat differ from our results published a decade ago, but they, nevertheless, lie within the limits of possible error of X_b calculation (± 0.1) indicated in the previous publication.[47]

Another interesting phenomenon is the behavior of the first coordination number ($N_1 + N_2$) shown in Figure 11, which reveals a maximum around 150−170 °C. This serves as a good illustration of our opinion that nothing extraordinary occurs at the points of maxima and minima in the temperature or pressure trends of water properties. It is obvious that the maximum of the first coordination number does not correspond to any qualitative change of the water structure. Moreover, the data presented in Figures 8, 9a, and 11 plainly show the reason for the maximum of half-width of ν_{OD}(HDO) discussed in section 2.

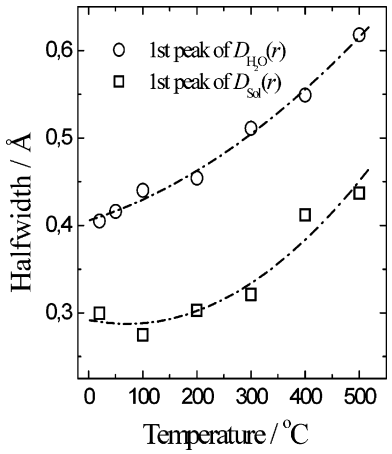

Figure 12. Half-width of the first peak of radial distribution of molecular density in water and NaCl solution.

The temperature trends for N_1 and N_2 in the NaCl solution (Figure 9b) are very different from the behavior of N_1 and N_2 for pure water. At room temperature, the number of molecules in the solution distributed around 3.2−3.3 Å is much larger than in water (4 against 1.5). This undoubtedly means a large contribution of O−H···Cl^- pairs to this distribution. Unlike the case of water, N_2 decreases monotonically with increasing temperature. The temperature dependence of N_1 for the solution is also different from that for pure water. Above 200 °C the decrease of N_1 is much slower. We can assume that such a difference in the behavior of two substances is a consequence of the phenomenon of *ion pairing* that will be discussed in the next section. Along with the usual process of the breaking of hydrogen bonds

$$\text{O}-\text{H}\cdots\text{O} \rightarrow \text{O}-\text{H} + \text{O}$$
$$(2.8\ \text{Å}) \rightarrow (3.2\ \text{Å})$$

the process of ion pair formation is taking place

$$\text{O}-\text{H}\cdots\text{Cl}^- + \text{Na}^+ \rightarrow \text{O}-\text{H} + \text{Cl}^-\text{Na}^+$$
$$(3.2\ \text{Å}) \rightarrow (2.8\ \text{Å})$$

which leads to the faster decrease of N_2 and more slower decrease of N_1 with increasing temperature along the isobar. The real situation is, of course, not that simple. The O−H groups may again form normal hydrogen bonds but as the temperature increases, the probability of H-bonding becomes lower.

Two important inferences may be drawn from this discussion. The higher the temperature, the more the properties of an electrolyte solution become nearer to the properties of pure water because in the first approximation one can consider ion pairs as neutral components of the solution. Another unexpected circumstance is that the energy characteristics of O−H···anion bonds are, most likely, close to the typical H-bonds in water, despite larger interatomic separations. This is how we can interpret the fact that the IR and Raman spectra of the solution and pure water show no substantial differences in the total energy of bonding.

Finally, the X-ray scattering results have shown that the structure of electrolyte solution is more ordered than the structure of pure water. The oscillations of the pair correlation functions of the solution are more pronounced than the $g(r)$ oscillations of water. Accordingly, the radius of correlation is also larger. In addition, as Figure 12 shows, the distribution of hydrogen-bonded O−O groups in the solution is by ∼25%

narrower than in water. Therefore, NaCl, being added to water, *does improve the short-range ordering of the hydrogen-bonded structure of bulk water* in the space between the coordination shells. We must admit that at the beginning of our work we looked at this possibility rather skeptically. This phenomenon can be probably explained by a stronger orientational correlation of $Cl^-\cdots H-O$ bonds and a lower mobility of water molecules coordinated to the ions, at least at lower temperatures.[36]

Despite the large difference between $g(r)$ of pure water and the solution, some remarkable features of the temperature behavior of water may be observed in the solution as well. It has been found, for example, that the H-bonding signature peak at ~4.5 Å in $g(r)$ of pure water practically disappears near the critical isotherm at isobaric heating.[24] Surprisingly, at higher temperatures the peak reappears and begins to grow again despite the fact that the degree of hydrogen bonding at 500 °C is very low. The average number of H-bonds per one molecule is ~1.1, as is seen in Figure 10. This curious phenomenon gave rise to an idea that hydrogen bonding in these high-temperature systems is associated with the formation of relatively short-lived H-bonded clusters of H_2O molecules that are locally quite ordered within the cluster, whereas the total number of H-bonds in the system still remains low, because most of the molecules are, nevertheless, not bonded at all. Computer simulations have recently proved the existence of rather large hydrogen-bonded clusters in supercritical water.[48,49] It is clearly seen in Figure 6 that the peak at ~4.5 Å in the pair correlation functions of the NaCl solution shows a similar behavior. It practically disappears at 300 °C but increases in amplitude again at 400 and 500 °C.

We are not discussing here the effects of dissolved Na^+ ion on the hydrogen-bonding structure of the solution. They are, of course, not less important than the interactions between water molecules and the anions. Unfortunately, no specific information about such interactions can be drawn directly from the experimental data presented here. Molecular dynamic computer simulations can help to clarify this important point.

5. MD Simulations and the Evidence of Ion Pairing in NaCl Solutions

It is well-known that the dielectric constant of water decreases dramatically with increasing temperature. This causes significant strengthening of the forces attracting oppositely charged ions in aqueous solutions. One may expect, therefore, the amount of "paired" ions to grow up at high temperatures.[50] That is an important phenomenon for it means that at high temperatures aqueous electrolyte solutions lose to some extent their "electrolytic" properties. This undoubtedly influences the properties of *hydrothermal fluid* in geological processes[51] and has to be taken into account in many applications of such a medium, for example, in the technologies supercritical water oxidation,[52] or crystal growth from supercritical solutions.[53]

However, first attempts to study the phenomena of ion pairing in electrolyte solutions on a truly atomistic level were made only recently, and linked to the development of the methods of molecular computer simulations for complex aqueous systems.[11−22] Although experimental techniques used in this work are unable to unambiguously prove the ion pair formation, computer simulations present a straightforward confirmation of this phenomenon.

We performed a total over 30 molecular dynamics (MD) simulation runs at temperatures and pressures from ambient to 500 °C and 1000 bar and for NaCl concentrations 0.55, 1.1, 2.2, and 4.4 M. A standard Hoover *NVT*-ensemble algorithm of MD simulations[54] was applied to a cubic simulation box that

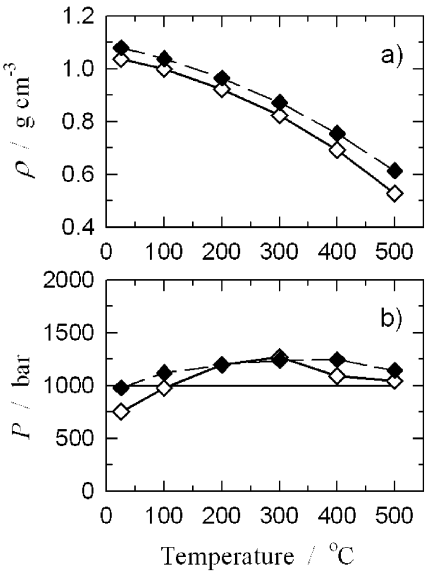

Figure 13. Temperature dependence of (a) density and (b) pressure for the thermodynamic states used in MD simulations. Open symbols: pure water. Filled symbols: 1.1 M aqueous NaCl solution.

contained 400 H_2O molecules and from 4 to 32 NaCl pairs, depending on the concentration. The densities of solution for each thermodynamic state simulated were chosen according to the equation of state for aqueous NaCl solutions valid over a wide range of temperatures, pressures, and concentrations.[30] For water−water interactions we used the simple point charge (SPC) intermolecular potential model.[55] This potential is one of the most frequently used models of water and is capable of producing reliable results in molecular simulations of a wide range of aqueous phases.[16,56,57] The parameters for ion−ion and ion−water interactions, consistent with the chosen water model, were taken from the previous work of Smith and Dang.[58,59] Periodic boundary conditions were applied, and a "spline cutoff" method was used to treat the short-range nonelectrostatic interactions, whereas all long-range electrostatic interactions were treated using the Ewald summation method.[54] A time step of 0.001 ps was used in all MD runs, and each equilibrium MD trajectory extended to 100 ps. To ensure the thermodynamic equilibrium in each run, the convergence of total energy and its components, as well temperature, pressure, and radial distribution functions for water and solution species, were carefully monitored during a 100 ps preequilibration period before the equilibrium MD trajectory was recorded for further statistical analysis.

The most detailed discussion of the MD results of this work will be published elsewhere.[60] Here, for consistency with the experimental data discussed above, we would like to concentrate only on the simulation results for one single concentration of 1.1 M and on the phenomena of ionic hydration and ion pairing, to complement this discussion. It is important to emphasize that the MD simulations were performed at a constant pressure of 1000 bar, but rather at constant volume corresponding to actual experimental densities at each temperature (Figure 13a). In this way the structural changes observed in the simulations could be more directly compared with experimental data obtained at the same densities as the simulations, despite the fact that the SPC model (like any other semiempirical molecular water model; e.g., refs 16, 56, and 57) does not exactly reproduce the *PVT* properties of water substance over a wide range of temperatures and pressures, and the actual pressures of each simulation run deviated somewhat from their nominal 1000 bar value (Figure 13b). It is also worth mentioning that upon heating from 25 to 500 °C at constant 1000 bar pressure, pure water

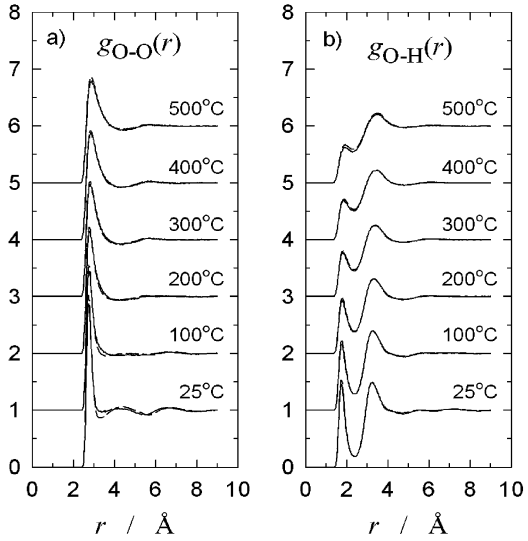

Figure 14. MD-simulated atom−atom radial distribution functions $O_{H_2O}-O_{H_2O}$ (a) and $O_{H_2O}-H_{H_2O}$ (b) in 1.1 M aqueous NaCl solution at different temperatures and at a constant pressure of 1000 bar. Dashed lines show the same distributions for pure water.

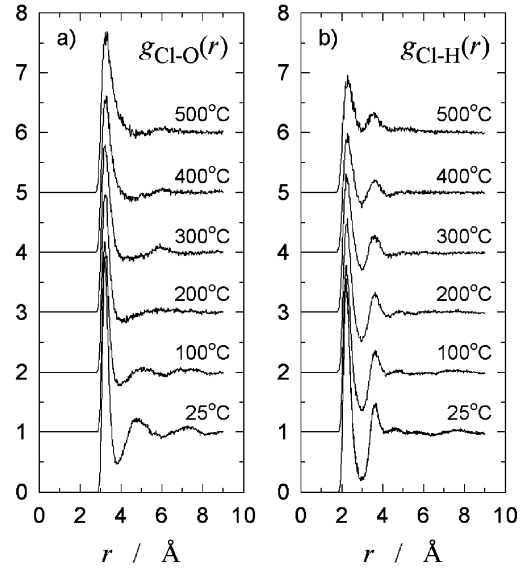

Figure 15. MD-simulated atom−atom radial distribution functions $Cl^- - O_{H_2O}$ (a) and $Cl^- - H_{H_2O}$ (b) in 1.1 M aqueous NaCl solution at different temperatures and at a constant pressure of 1000 bar.

expands by 96% (from 1.0373 to 0.52832 g/cm^3), whereas the 1.1 M NaCl solution under the same thermodynamic conditions expands by only 76% (from 1.0798 to 0.613283 g/cm^3).

Figures 14−16 show the evolution of simulated atom−atom radial distribution functions characterizing the local structure around H_2O molecules, Cl^- ions, and Na^+ ions, respectively. They are all in good qualitative agreement with the results of other computer simulations[11−21] and neutron diffraction experiments[7−9] at similar elevated temperatures and pressures. To compare these results with the X-ray diffraction data in Figure 6, we should keep in mind that all six atom−atom radial distribution functions contribute to the experimentally observed X-ray scattering function. A comparison of the simulated individual atom−atom contributions to the total pair correlation function clearly shows that the only possible explanation for the temperature evolution of this function observed in Figure 6b can be the significant increase of the Na^+-Cl^- pair correlation (at ∼3 Å in Figure 16b) with increasing temperature. It is now well established that the ion−ion interactions become

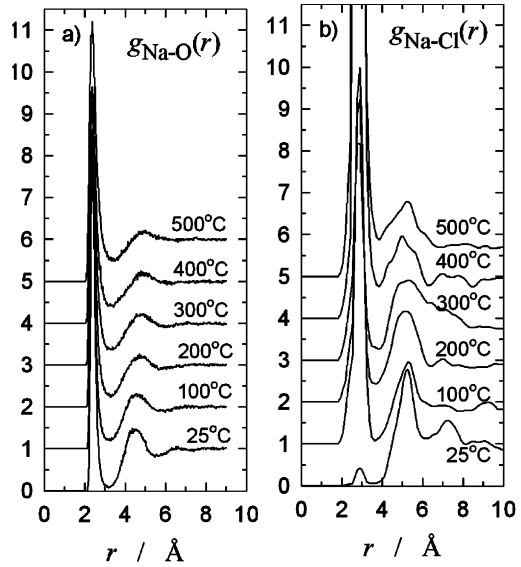

Figure 16. MD-simulated atom−atom radial distribution functions $Na^+-O_{H_2O}$ (a) and Na^+-Cl^- (b) in 1.1 M aqueous NaCl solution at different temperatures and at a constant pressure of 1000 bar.

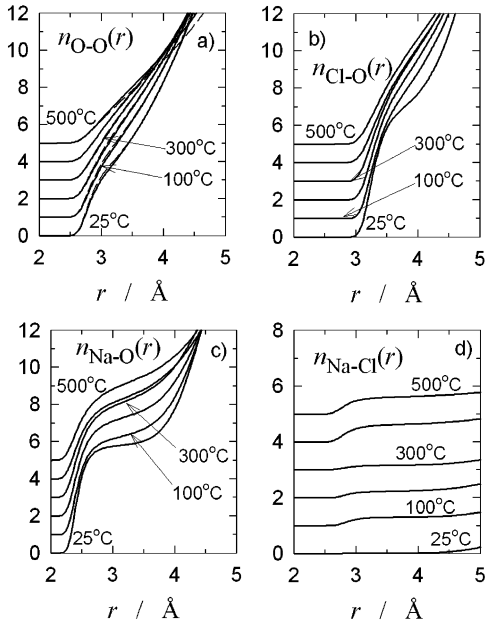

Figure 17. Running coordination numbers characterizing the local structural environments of H_2O, Cl^-, and Na^+ in a 1.1 M aqueous NaCl solution at different temperatures and at a constant pressure of 1000 bar. The curves are shifted by +1.0 with increasing temperature. Dashed lines in (a) show the same functions for pure water.

increasingly important in determining the structure and properties of electrolyte solutions at high-temperatures.[11−21]

Figure 17a−d shows the running coordination numbers, $n_{ij}(r)$, calculated from the $g_{ij}(r)$ functions in Figures 14−16 for the nearest neighborhood of the H_2O molecules, Na^+, and Cl^- as

$$n_{ij}(r) = 4\pi\rho_j \int_0^r g_{ij}(r) r^2 \, dr \qquad (3)$$

where ρ_j is the number density of species j in the system. Interestingly, the $g_{O-O}(r)$, $g_{O-H}(r)$, $n_{O-O}(r)$, and $n_{O-H}(r)$ functions of the NaCl solutions are almost indistinguishable from those of pure water under the same conditions (dashed lines in Figures 14a,b, and 17a). Accordingly, the number of H_2O

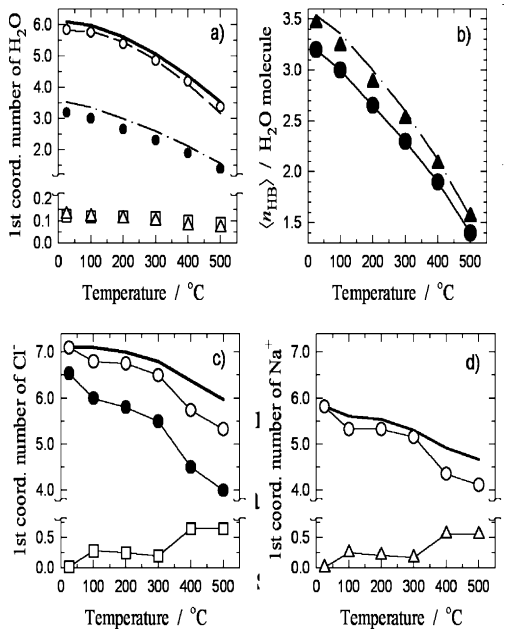

Figure 18. Temperature dependence of the compositional changes in the nearest-neighbor environment of (a) H_2O, (c) Cl^-, and (d) Na^+ in a 1.1 M aqueous NaCl solution at a constant pressure of 1000 bar. (b) Average number of H-bonds per water molecule in the system. Thick solid lines in (a), (b), and (d): total coordination numbers. Open squares: coordination by Na+ ions. Open triangles: coordination by Cl^- ions. Open circles: coordination by H_2O molecules. Filled circles: H-bonded nearest H_2O molecules (dashed and dash−dotted lines in (a) and (b) show the same functions for pure water). Filled triangles in (b): total number of H-bonds per H_2O molecule in the solution, including the contribution of H-bonds donated to Cl^- ions. Symbol size corresponds to the estimated accuracy of calculations.

molecules coordinating other H_2O molecules is essentially identical for both systems at all thermodynamic conditions.

Figure 18 shows the temperature evolution of the number of H_2O, Cl^-, and Na^+ in the first coordination sphere of these species obtained from the MD simulations and the number of H-bonded water molecules contributing to the coordination spheres of H_2O and Cl^-. The cutoff distances of the first coordination spheres were defined as 3.6, 3.9, and 3.2 Å for H_2O, Cl^-, and Na^+, respectively, on the basis of the positions of the minima in the corresponding radial distribution functions in Figures 14−16. The criteria applied to define the existence of a hydrogen bond are those frequently used in the analysis of the liquid water structure: intermolecular A···H distances less than a certain $R_{A\cdots H}$ value and angles, β, between the A···O and O−H vectors less than 30°.[61] "A" here denotes the acceptor of H-bonds, which can be either O_{H_2O} or Cl^-, and the threshold values of $R_{O\cdots H} = 2.4$ Å and $R_{Cl\cdots H} = 3.0$ Å were used because they correspond to the positions of the first minima in the respective A−H radial distribution functions (Figures 14b and 15b). The angular threshold of $\beta \leq 30°$ is known to cover ∼90% of the distribution of H-bonding angles in bulk liquid water under ambient conditions.[61]

Although the average total number of neighbors in the first coordination shell of each Cl^- ion decreses only from 7.0 to 6.0 between the lowest and the highest temperatures studied (thick solid line in Figure 18c), the average number of H_2O molecules there decreases down to 5.3 (open circles in Figure 18c), and they remain donating only 4.3 H-bonds to the Cl^- ion, compared to 6.5 at room temperature (filled circles in Figure 18c). Similarly, the average number of H_2O molecules coordinating Na^+ ions drops from 5.8 to 4.1 (Figure 18d). However, in both cases this dilution in coordination by the solvent is somewhat compensated by the increased presence of the counterions in the first coordination sphere. At room temperature, there is a noticeable, though quite negligible fraction of Na^+Cl^- ion pairs formed in the solution resulting in only ∼0.02 counterions on average present in the first coordination shell. This situation changes dramatically with increasing temperature. Already at 100 °C there are, statistically, 0.2−0.3 Cl^- ions around each Na^+, and vice versa, indicating a significant fraction of Na^+Cl^- ion pairs present in the solution. This fraction remains more or less the same until at the constant pressure the temperature rises above 300 °C. (Due to the relatively small number of ions in the system, we estimate that the statistical accuracy of our $n(r)$ calculations is on the order of 0.1. Therefore, we are making no attempt to interpret a potentially interesting trend of a slight decrease in the degree of ion pairing in the solution with increasing temperatures between 100 and 300 °C). At supercritical temperatures of 400 and 500 °C the simulated picture of ion pairing changes even more dramatically. Now nearly 0.6 ions have at least one of the oppositely charged ions in their nearest neighborhood. Moreover, under these conditions the number of nearest-neighbor like-charged ions (Na^+Na^+, Cl^-Cl^-) also increases by a factor of 2−4 (figure not shown), clearly indicating the occasional formation not only of ion pairs but also of larger multiionic clusters under these conditions. These results are in good agreement with previous molecular simulations of the degree of ion pairing and ion association in supercritical aqueous solutions for the same system under somewhat different thermodynamic conditions[11−21] and allow us to estimate that approximately 75 ± 10% of ions in aqueous NaCl solution are associated at 500 °C and 1000 bar.

The total number of accepted and donated H-bonds formed by each water molecule with its neighboring H_2O is always lower in the solution (filled circles in Figure 18b) than in pure water under the same conditions (dash−dotted line in Figure 18b). However, if the H-bonds donated to Cl^- ions are additionally taken into account (filled triangles in Figure 18b), the numbers of H-bonds per water molecule in the system become nearly identical between pure water and NaCl solution. Comparing the positions of the first peak in Figures 14b and 15b, it is clear that the $Cl^-\cdots H$ bonds are, on average, somewhat longer than the O···H bonds between H_2O molecules. However, this does not give rise to weaker bonds, because the enlarged H-bonding distances are nearly exactly compensated by stronger $Cl^-\cdots H$ electrostatic attraction (O_{H_2O} bears a partial charge of $-0.82|e|$ in the SPC water model vs full formal charge of $-1|e|$ of the Cl^-). Thus, both the average number and the average strength of H-bonds formed by each H_2O molecule remain nearly the same in the 1.1 M NaCl solution as in pure water at all temperatures. This explains the peculiar behavior of their vibrational spectra observed in Figures 1 and 4.

6. Conclusions

In this work, we attempted to answer some of the key questions concerning the structure and properties of electrolyte solutions. The study has revealed the important fact that any analytical technique taken alone cannot lead to the adequate understanding of the complex phenomena, taking place in such solutions over a wide range of temperatures, pressures, and concentrations. For example, if we had restricted ourselves to the vibrational spectroscopy only, we would have arrived at a wrong conclusion that a salt added to water does not at all influence the hydrogen bonding and the structure of the fluid. This might, indeed, explain the observation of the negligible

effect of ions on the H-bonding structure of liquid water probed by vibrational spectroscopy.[62] Our present spectroscopic and MD observation that the energy characteristics of $Cl^-\cdots H-O-H$ bonds are, most likely, close to those of the typical H-bonds in the solvent water (despite somewhat larger interatomic separations), meets, in fact, a fairly unexpected corroboration in the results or recent MD simulations of the energetics, structure, and dynamics of Cl^- ions in various hydrated environments, such as on the surface of hydrous minerals, or in the hydrous interlayers of clay-like phases.[63−67]

On the other hand, the X-ray diffraction data taken alone would have induced one to believe that the distribution of energy of intermolecular interactions in pure water and NaCl solution should be very different, which is, of course, not so. Finally, without MD simulations we would have hardly been able to understand and interpret the entire molecular-scale picture of the observed phenomena and the reasons for the above seemingly contradictive interpretations. Only combined use of several complementary methods for the same substance at identical thermodynamic conditions allows us to achieve the better understanding of the behavior of electrolyte solutions at high temperatures and pressures. Perhaps, this is the most important conclusion we can draw from this work.

Acknowledgment. This research was supported by by the Russian Foundation for Basic Research (Grants 03-05-64332 and 03-03-32950), INTAS (Grant 00-0640), the U.S. Department of Energy (Basic Energy Sciences, Grant DEFGO2-00ER-15028), and the NSF Science and Technology Center of Adwanced Materials for Water Purification *WaterCAMPWS* (Grant 0120978) at the University of Illinois. The computations were partially supported by the National Computational Science Alliance (Grant EAR 990003N) and utilized NCSA SGI/CRAY Origin2000 computers and Cerius2-4.6 software package from *Accelrys*. We thank R. James Kirkpatrick for many useful discussions.

References and Notes

(1) Shaw, R. V.; Brill, T. B.; Clifford, A. A.; Eckert, C. A.; Franck, E. U. *Chem. Eng. News* **1991**, *69*, 26.

(2) Darr, J. A.; Poliakoff, M. *Chem. Rev.* **1999**, *99*, 495.

(3) Ohtaki, H.; Radnai, T. *Chem. Rev.* **1993**, *93*, 1157.

(4) Enderby, J. E.; Neilson, G. W. *Rep. Prog. Phys.* **1981**, *44*, 593.

(5) Marcus, Y. *Chem. Rev.* **1988**, *88*, 1475.

(6) Simonson, J. M.; Palmer, D. A. *Geochim. Cosmochim. Acta* **1993**, *57*, 1.

(7) Powell, D. H.; Neilson, G. W.; Enderby, J. E. *J. Phys. Condens. Matter* **1993**, *5*, 5723.

(8) de Jong, P. H. K.; Neilson, G. W. *J. Chem. Phys.* **1997**, *107*, 8577.

(9) Yamaguchi, T.; Soper, A. K. *J. Chem. Phys.* **1999**. *110*, 3529.

(10) Dubessy, J.; Rull-Perez, F. *Proc Joint ISHR & ICSTR* **2000**, 72.

(11) Cui, S. T.; Harris, J. G. *Chem. Eng. Sci.* **1994**, *49*, 2749.

(12) Chialvo, A. A.; Cummings, P. T.; Cochran, H. D.; Simonson, J. M.; Mesmer, R. E. *J. Chem. Phys.* **1995**, *103*, 9378.

(13) Johnston, K. P.; Bennet, G. E.; Balbuena, P. B.; Rossky P. J. *J. Am. Chem. Soc.* **1996**, *118*, 6746.

(14) Driesner, T.; Seward, T. M.; Tironi, I. G. *Geochim. Cosmochim. Acta* **1998,** *62*, 3095.

(15) Brodholt, J. P. *Chem. Geol.* **1998**, *151*, 11.

(16) Chialvo, A. A.; Cummings, P. T. *Adv. Chem. Phys.* **1999**, *109*, 115.

(17) Reagan, M.; Harris, J. G.; Tester, J. W. *J. Phys. Chem. B* **1999**, *103*, 7935.

(18) Mountain, R. D. In *Steam, Water, and Hydrothermal Systems. Physics and Chemistry Meeting the Needs of Industry*; Tremaine, P. R., et al., Eds.; NRC-CNRC: Ottawa, Canada, 2000; pp 509−516.

(19) Koneshan, S., Rasaiah, J. C. *J. Chem. Phys.* **2000**, *113*, 8125.

(20) Koneshan, S.; Rasaiah, J. C.; Dang, L. X. *J. Chem. Phys.* **2001**, *114*, 7544.

(21) Sherman, D. M.; Collings, M. D. *Geochem. Trans.* **2002**, *3*, 102.

(22) Tongraar, A.; Rode, B. M. *Chem. Phys. Lett.* **2004**, *385*, 378

(23) Dogonadze, R. G., et al., Eds. *The Chemical Physics of Solvation;* Elsevier: Amsterdam, 1985; Parts a−c.

(24) Gorbaty, Y. E.; Gupta, R B. *Ind. Eng. Chem. Res.* **1998**, *290*, 63.

(25) Eisenberg, D.; Kauzman, W. *The Structure and Properties of Water*; Oxford University Press: Oxford, NY, 1969.

(26) Gorbaty, Yu. E.; Bondarenko, G. V. *Appl. Spectrosc.* **1999**, *53*, 908.

(27) Gorbaty, Yu. E.; Bondarenko, G. V.; Venardou, E.; Barlow, S. J.; Garcia-Verdugo, E.; Poliakoff, M. *Vibr. Spectrosc.* **2004**, *35*, 97.

(28) Zarembo, V. I.; Feodorov, M. R. *Zh Prikl. Khim.* **1975**, *48*, 1949.

(29) Gehrig, M.; Lentz, H.; Franck, E. U. *Ber. Bunsen-Ges. Phys. Chem.* **1983**, *87*, 597.

(30) Lvov, S. N.; Wood, R. H. *Fluid Phase Equilib.* **1990,** *60*, 273.

(31) Wagner, W.; Pruss, A. *J. Phys. Chem. Ref. Data* **2002**, *31*, 387.

(32) Pimentel, G. C.; McClellan, A. L. *The hydrogen bond*; Freeman: San Francisco, 1960.

(33) Sokolov, N. D. *Zh. Vses. Khim. Ova.* **1972**, *17*, 299 (in Russian).

(34) Gorbaty, Yu. E.; Bondarenko, G. V. *J. Supercrit. Fluids* **1998**, *14*, 1.

(35) Kropman, M. F.; Bakker, H. J. *Chem. Phys. Lett.* **2003**, *370*, 741.

(36) Kropman, M. F.; Bakker, H. J. *Science* **2001**, *291*, 2118.

(37) Scherer, J. R. *Advances in infrared and Raman spectroscopy*; Heyden: Philadelphia, 1978.

(38) Okhulkov, A. V.; Gorbaty, Yu.E. *J. Mol. Liq.* **2001**, *93*, 39.

(39) Giessen, B. C.; Gordon, G. E. *Science* **1968**, *159*, 973.

(40) Gorbaty, Yu.E.; Demianets, Yu. N. *Mol. Phys* **1985**, *55*, 571.

(41) Gorbaty, Yu. E.; Demianets, Yu. N. *Zh. Strukt. Khim.* **1982**, *23*, 882 (in Russian).

(42) Gorbaty, Yu. E.; Demianets, Yu. N. *Zh. Strukt. Khim.* **1983**, *24*, 716 (in Russian).

(43) Okhulkov, A. V.; Demianets, Yu. N.; Gorbaty, Yu. E. *J. Chem. Phys.* **1994**, *100*, 1578.

(44) Kaspar, J. S., Lonsdale, K., Eds. *International Tables of Crystallography*; Kynoch: Birmingham, 1962; Vol. 3.

(45) Narten, A. H.; Levy, H. A. *J. Chem. Phys.* **1971**, *55*, 2263.

(46) Narten, A. H.; Venkatesh, G. C.; Rice, S. A. *J. Chem. Phys.* **1976**, *64*, 1106.

(47) Gorbaty, Yu. E.; Kalinichev, A. G. *J. Phys. Chem.* **1995**, *99*, 5336.

(48) Kalinichev, A. G.; Churakov, S. V. *Chem. Phys. Lett.* **1999**, *302*, 411.

(49) Kalinichev, A. G.; Churakov, S. V. *Fluid Phase Equilib.* **2001**, *183*, 271.

(50) Oelkers, E. H.; Helgeson, H. C. *Science* **1993,** *261*, 888.

(51) Seward, T. M.; Barnes, H. L. In *Geochemistry of Hydrothermal Ore Deposits*, Barnes, H. L., Ed.; John Wiley & Sons: New York, 1997; pp 435−486.

(52) Akiya, N.; Savage, P. E. *Chem. Rev.* **2002,** *102*, 2725.

(53) Balitsky, V. S.; Balitskaya, L. V.; Kalinichev, A. G.; Marina, E. A.; Iwasaki, H.; Iwasaki, F. *J. Supercrit. Fluids* **1998**, *13*, 357.

(54) Allen, M. P.; Tildesley, D. J. *Computer Simulation of Liquids*; Oxford University Press: New York, 1987.

(55) Berendsen, H. J. C.; Postma, J. P. M.; Van Gunsteren, W. F.; Hermans, J. *Intermolecular Forces*; Riedel: Dordrecht, The Netherlands, 1981.

(56) Kalinichev, A. G. *Rev. Mineral. Geochem.* **2001**, *42*, 83.

(57) Guillot, B. *J. Mol. Liq.* **2002**, *101*, 219.

(58) Smith, D. E.; Dang, L. X. *J. Chem. Phys.* **1994**, *100*, 3757.

(59) Dang, L. X. *J. Am. Chem. Soc.* **1995**, *117*, 6954.

(60) Kalinichev, A. G.; Gorbaty, Yu. E.; Kirkpatrick, R. J. Manuscript in preparation.

(61) Luzar, A. *J. Chem. Phys.* **2000**, *113*, 10663.

(62) Omta, A. W.; Kropman, M. F.; Woustersen, S.; Bakker, H. J. *Science* **2003**, *301*, 347.

(63) Kalinichev, A. G.; Kirkpatrick, R.J. *Chem. Mater.* **2002**, *14*, 3539.

(64) Kalinichev, A. G.; Kirkpatrick, R. J.; Cygan, R. T. *Am. Miner.* **2000**, *85*, 1046.

(65) Kirkpatrick, R. J.; Kalinichev, A. G.; Wang, J.; Hou, X.; Amonette, J. E. In *The Application of Vibrational Spectroscopy to Clay Minerals and Layered Double Hydroxides*; Kloprogge, J. T., Ed.; *Clay Minerals Society Workshop Lectures*; The Clay Minerals Society: Aurora, CO, 2005; Vol. 13, pp 239−285.

(66) Wang. J.; Kalinichev A. G.; Amonette, J. E.; Kirkpatrick, R. J. *Am. Miner.* **2003**, *88*, 398.

(67) Hou, X.; Kalinichev, A. G.; Kirkpatrick, R. J. *Chem. Mater.* **2002**, *14*, 2078.